# Aircraft and ground-based measurements of hydroperoxides during the 2006 MILAGRO field campaign

L. J. Nunnermacker, J. B. Weinstein-Lloyd, B. Hillery, B. Giebel, L. I. Kleinman, S. R. Springston, P. H. Daum, J. Gaffney, N. Marley, G. Huey

**Atmospheric
Chemistry
and Physics
Discussions**

**Hydroperoxides in
MILAGRO, 2006**

L. J. Nunnermacker et al.

# Aircraft and ground-based measurements of hydroperoxides during the 2006 MILAGRO field campaign

**L. J. Nunnermacker[1], J. B. Weinstein-Lloyd[2], B. Hillery[2], B. Giebel[3],
L. I. Kleinman[1], S. R. Springston[1], P. H. Daum[1], J. Gaffney[4], N. Marley[4], and
G. Huey[5]**

[1]Brookhaven National Laboratory, Atmospheric Sciences Division, Upton, NY 11973, USA
[2]Chemistry/Physics Department, State University of New York, Old Westbury, NY 11568, USA
[3]Rosenstiel School of Marine and Atmospheric Science, Div. of Marine and Atmospheric
Chemistry, Univ. of Miami, Miami, FL 33149, USA
[4]University of Arkansas, Department of Chemistry, Little Rock, AR 72204, USA
[5]Georgia Inst. of Technol., School of Earth & Atmospheric Sciences, Atlanta, GA 30332, USA

Correspondence to: L. J. Nunnermacker (lindan@bnl.gov)

| | |
|---|---|
| | Title Page |
| Abstract | Introduction |
| Conclusions | References |
| Tables | Figures |
| ◄◄ | ►► |
| ◄ | ► |
| Back | Close |
| Full Screen / Esc | |
| Printer-friendly Version | |
| Interactive Discussion | |

## Abstract

Mixing ratios of hydrogen peroxide and hydroxymethyl hydroperoxide were determined aboard the US Department of Energy G-1 Research Aircraft during the March 2006 MILAGRO field campaign in Mexico. Ground measurements of total hydroperoxide were made at the T1 site at Universidad Technologica de Tecámac, about 35 km NW of Mexico City. In the air and on the ground, peroxide mixing ratios near the source region were generally near 1 ppbv, much lower than had been predicted from photochemical models based on the 2003 Mexico City study. Strong southerly flow resulted in transport of pollutants from the T0 to T1 and T2 surface sites on several flight days. On these days, it was observed that peroxide concentrations slightly decreased as the G-1 flew progressively downwind. This observation is consistent with low or negative net peroxide production rates calculated for the source region and is due to the very high $NO_x$ concentrations above the Mexico City plateau. However, relatively high values of peroxide were observed at takeoff and landing near Veracruz, a site with much higher humidity and lower $NO_x$ concentrations.

## 1 Introduction

In March 2006, MILAGRO (Megacity Initiative: Local and Global Research Observations) an international and multi-agency field experiment took place with the primary goal of learning how a megacity affects air quality. Air pollution generated by megacities (i.e., population >10 million) is an important environmental, health, and financial issue facing many urban areas (Molina and Molina, 2002). In addition to the local effects, there is the potential for the growing number of megacities to have global impact on air quality as well as climate change. Mexico City is uniquely situated on an elevated basin (2240 m m.s.l. – mean sea level) surrounded by mountains with openings to the north and south-southwest. This large city has diverse sources of fossil fuel combustion, including automotive (nearly 4 million vehicles), residential cooking and

heating, and various industries providing ample amounts of hydrocarbons and oxides of nitrogen.

The Department of Energy (DOE) portion of MILAGRO, the Megacity Aerosol eXperiment – MEXico City (MAX–Mex) focused on the chemical, physical, and optical characterization of aerosols, as well as trace gas precursors of aerosols and photochemistry. The DOE G-1 aircraft flew in and around the city source region (MCMA=Mexico City Metropolitan Area) and into the outflow from the city in an effort to study the effects of the megacity plume. The field program was designed so that investigators could follow the outflow of the source region (T0 site – central Mexico City) as it moved over two downwind sites (T1 – Tecamac University ~35 km from T0, and T2 – Rancho la Bisnaga ~70 km from T0) (Doran, 2007).

Peroxides are important termination products of the free-radical chemistry responsible for ozone formation in the troposphere. Under low $NO_x$ conditions, combination reactions of peroxy radicals ($HO_2$ and $RO_2$) leading to hydroperoxides ($H_2O_2$ and $ROOH$) are the primary termination pathway for the ozone ($O_3$) forming chain reaction. Under high $NO_x$ (nitric oxide and nitrogen dioxide; $[NO+NO_2]$) conditions, concentrations of $HO_2$ and $RO_2$ are suppressed by reactions with NO. The primary termination pathway is then by reaction of free radicals with $NO_x$ leading to compounds collectively designated as $NO_z$ that include nitric acid ($HNO_3$), organic nitrates, and peroxyacetyl nitrates (PANs). Photochemical model calculations show that ozone production is $NO_x$- or VOC-limited according to whether it occurs under low or high $NO_x$ conditions, or equivalently according to whether peroxides or $NO_z$ are the primary termination products (Sillman, 1995; Kleinman, 2001, 2005a). The ratio of $H_2O_2$ to $HNO_3$ therefore indicates whether $O_3$ was formed in a $NO_x$- or VOC-limited environment and can be used to develop $O_3$ mitigation strategies (Sillman, 1995, 1999; Watkins et al., 1995).

In comparison to other cities in which the G-1 has been used for urban sampling, $NO_x$ concentrations over downtown Mexico City are extremely high (Kleinman et al., 2005b). Concentrations at 500 m altitude (a.g.l. – above ground level) approach 100 ppbv, a value usually seen only in power plant plumes. Under these conditions it is expected

that peroxide formation will be suppressed and $O_3$ production will be strongly VOC limited. Peak $O_3$ levels, however, occur in the afternoon under lower $NO_x$ conditions in areas that are downwind of the City. The usual sequence of events is for photochemistry to start out VOC limited and become $NO_x$ limited as an air mass ages (Kleinman et al., 2001). There is little observational evidence as to where and when this transition occurs in Mexico City and how it affects peak $O_3$ levels.

In place of direct observational evidence, models have been used to determine whether peak $O_3$ concentrations in Mexico City can be more effectively controlled by reducing $NO_x$ or VOC emissions (Lei et al., 2007). Models typically are validated by their performance in predicting concentrations of $O_3$ and a few other commonly measured species. It is not uncommon for such models to correctly predict ozone, while failing to correctly predict concentrations of the peroxide and $HNO_3$ radical termination products. From the standpoint of developing $O_3$ control strategies, it is important that models properly represent the chemical pathways associated with $NO_x$ and VOC limited conditions. Accurate $H_2O_2$ observations and model predictions of $H_2O_2$ are important in distinguishing between these pathways.

The MILAGRO campaign was the first instance in which peroxides were measured in Mexico City. This study presents observations from the T1 surface site and the G-1 aircraft using a glass coil inlet scrubber with continuous flow derivatization and fluorescence detection (Lee et al., 1990, 1994). G-1 flights were directed primarily at measurements over Mexico City and downwind areas on the Mexico City plateau. Ferry segments to and from Veracruz, located in a more humid, less polluted environment 300 km to the east on the Gulf of Mexico, provide an interesting contrast to the observations taken over the plateau.

## 2  Experimental

### 2.1  Meteorological conditions and G-1 flights

A trajectory analysis by Doran et al. (2007) indicates the days when pollutants from Mexico City were likely to impact the T1 and T2 ground sites (Table 1). The peroxide instrument was operational on nine of the G-1 flights. Five of which were on 18, 19, and 20 March with transport from Mexico City to T1 and T2. Several other days had briefer periods of flow from the urban region to these ground sites (i.e., 26 and 27 March). In some cases, the air traveling over the surface sites did not originate in the urban basin (i.e., 15 March). Also observed was a distinct change in the relative humidity on 21st March, thus separating the field experiment into a dry period (1–20 March) and a wet period (21–28 March). Boundary layer behavior and heights appeared to be similar at T1 and T2 (i.e., 1000–3500 m a.g.l. from 11:00–15:00 LST, respectively), these values were slightly lower than in a previous campaign (Doran et al., 1998, 2007).

The DOE G-1 Research Aircraft was based at sea level and operated from the General Heriberto Jara International Airport in Veracruz, Mexico. Starting on 3 March 2006 through the end of the month, the DOE G-1 flew 15 research flights during the MILAGRO field campaign. On the G-1, peroxide measurements were made on every flight starting on the afternoon of 15 March through 27 March 2006. All results reported in this paper use only the data subset for this period of time. Typically, there was a morning flight track around the source region (L3, L4, L5), over the source region (L0) and sometimes downwind over L1 and L2, see Fig. 1. In the afternoon, the flight track was usually repeated over L0 and then sampled the urban plume farther downwind over L1 and then L2 (see Fig. 1). For a description of trace gas and particle instrumentation aboard the G-1, the reader is directed to Springston, 2006.

## 2.2   G-1 Peroxide measurements

Hydroperoxides were captured by passing sampled air over an aqueous surface film in a glass coil scrubber, followed by continuous-flow derivatization, and fluorescence detection. Three independent channels, using different reagents, were used to allow detection of the dissolved hydroperoxides, as summarized in Table 2. Details of the collection and analysis system can be found in the references (Lee et al., 1990, 1994). Due to the high altitude required for flights over Mexico City, we reconfigured the peroxide analyzer for operation in a pressurized cabin. The inlet was designed to minimize contact of sampled air with dry surfaces prior to scrubbing. Ram air was directed through a 45° forward-facing 1/2″ ID bypass, and drawn through 4.2″ of $^1/_4$″ OD tubing prior to meeting scrub solution. A diaphragm pump was used to draw air at 1.5 SLPM through each channel using individual mass flow controllers. Surfaces exposed to the air sample stream were either glass or Teflon® PFA tubing. Baselines were established prior to and during flight using zero air.

Two-point calibrations were conducted before or after each flight using aqueous peroxide standards, nominally 2.0 and 4.0 or 4.0 and 8.0 $\mu$M, prepared from unstabilized 3% peroxide stock, with scrubbing solution used for the final dilution. Stock peroxide was titrated against standardized permanganate before and after the 30-d measurement period, and no decrease in concentration was observed. Liquid and air flow rates, nominally 0.6 mL/min and 1.5 L/min, respectively, were calibrated regularly.

A 4-channel filter fluorimeter system with dual cadmium lamps and 24 $\mu$L flow-through fluorescence cells (McPherson, Inc., Chelmsford, MA) was used for the first time in this study. The 10–90% response time of the instrument was 42 s. The detection limit, based on 2x the baseline noise, was 0.27 ppbv for $H_2O_2$ and 0.38 ppbv for HMHP. Only measurements of HMHP and $H_2O_2$, obtained from channels 2 and 3, are reported here. A leak in channel 1 prevented us from acquiring a reliable baseline for the total soluble peroxide concentration, which is also needed to make the difference measurement for methyl hydroperoxide.

Aircraft data for the MAX–Mex field program may be obtained at the following URL: ftp://ftp.asd.bnl.gov/pub/ASP%20Field%20Programs/2006MAXMex/. Unless otherwise noted, all G1 data used in this paper were 10-s averages.

## 2.3 T1 Ground measurements

Hydroperoxide measurements were conducted at Universidad Technologica de Tecámac, a surface site about 35 km NW of Mexico City at an elevation of 2.3 km. Because the site abutted a 4-lane highway, and was located less than 1 km from a farm, it was impacted by motor vehicle and $NH_3$ emissions on a regular basis. Trajectory analyses show that this site was downwind of Mexico City for approximately half of the days between 15th March and 30th March (Doran et al., 2007). A continuous peroxide analyzer was deployed in the Georgia Tech trailer at the surface site. We measured only total soluble peroxide, using pH 9 scrubbing solution and POHPAA-derivatizing reagent, as described above for the aircraft measurements. Earlier studies have shown that there is potential for substantial loss of peroxide in inlet lines during surface sampling (Jackson et al., 1996; Lee et al., 1991; Watkins et al., 1995). To avoid inlet losses, we mounted the coil scrubbers on the trailer roof approximately 5 m above the ground, and drew air through a pinhole directly into the stripping solution. The resulting aqueous peroxide solution was pumped to the instrument through 2 m of 0.8 mm ID PFA tubing. Previous laboratory tests showed no peroxide decomposition in the aqueous solution under these conditions. However, this arrangement creates significant lag time between collecting and observing sample (12 min), and a somewhat broadened response (10–90% rise time of 2.0 min). Data reported here were corrected for the lag time, and ten-minute averages were used for all data analysis. The liquid flow rate was maintained nominally at 0.3 mL/min using a peristaltic pump, and the air flow at 1 LPM using a critical orifice. Liquid and air flow rate calibrations were conducted three times during the measurement period. The local pressure at this site (0.77 atm) was used to compute the equivalent gas-phase concentration. Two-point calibrations were conducted daily using aqueous peroxide standards, nominally 2.0 and 4.0 $\mu$M,

Full Screen / Esc

Printer-friendly Version

Interactive Discussion

prepared from unstabilized 3% peroxide stock, with scrubbing solution used for the final dilution. The detection limit for this configuration was 0.27 ppbv, based on twice the baseline noise. All ground data may be obtained on the NCAR data portal at the following URL (registration required): http://cdp.ucar.edu/home/home.htm.

## 3 Observations

### 3.1 G-1

#### 3.1.1 General flight statistics

In this section, we present peroxide observations from 15–27 March 2006. Shown in Fig. 1 is a composite of all the flight legs around the source region (L3, L4, L5), the source leg (L0 over T0) and the outflow legs (L1 over T1 and L2 over T2). Listed in Table 3, according to leg, are the means and maximums for 8 flights listed. The average peroxide and HMHP concentrations, for the entire period over all the regions, were low (i.e., $\leq 1.6$ and $\leq 0.37$ ppbv, respectively) with no significant increase even over L2. On the other hand, the $NO_x$ concentrations were quite high in the source region (i.e., $\geq 23$ ppbv) and then decreased as the air flowed over L1 and L2. From these data, it is also apparent that legs L3 and L4 were actually part of the source region with average values for $O_3$, $NO_y$ and CO similar to those of T0. Most of the time, L5 had much lower average concentrations of the criteria pollutants and is considered to be background air.

### 3.2 Vertical distributions

Composite vertical distributions for several species of interest are shown in Fig. 2. Measurements were made upon take-off from and descent into the Veracruz Airport as well as over the Mexico City basin. Altitudes between 0–500 m are not shown due to the fact

that some instruments were not turned on until the G-1 was airborne and concentration extremes at ground level in the airport. Altitudes lower than 2500 m are limited to periods when the G-1 had taken off from or was on approach to the airport at Veracruz. The 2500–3000 m altitude bin primarily contains data from traverses over Mexico City on L0 and surrounding areas (L3, L4, and L5). At 3000 and 3500 m there is a mixture of contribution from all legs except L2. At higher altitudes, above 3500 m, most of the data are from L1 and L2. Median CO and $NO_y$ concentrations were the largest between the altitudes of 2500 and 3000 m (i.e., over the source region). Median $O_3$ concentrations slightly increased between the altitudes of 2500 to 4000 m indicating that ozone is produced as air masses move downwind. Sulfur dioxide, $SO_2$, concentrations (not shown in the figure) were dominated by the large excursions observed while flying over the Tula power plant ($20°06'13.23''$, $-99°17'07.16''$). After removing $SO_2$ plume data (peak concentrations >100 ppbv), we observed the highest $SO_2$ concentrations in the MCMA region.

Although our primary goal was to study emissions and transformations in and around the Mexico City region, we note here some interesting features from measurements conducted in and around Veracruz at altitudes <2500 m. The median water vapor concentration peaked between 500 and 1000 m and decreased with increasing altitude (Fig. 2). Concentrations of $NO_y$ were relatively low (median value less than 4 ppbv) and consisted of less than 20% $NO_x$. The highest median and maximum peroxide concentrations for the entire campaign were observed in this region. HMHP concentrations (not shown in Fig. 2) varied little with altitude and were essentially at the detection limit for the entire program. These observations are consistent with our understanding of the mechanism of $H_2O_2$ formation in a high-humidity and low-$NO_x$ environment.

3.2.1 Production of peroxide

In the free troposphere, where $NO_x$ is low and there are no depositional losses, we expect peroxide concentration to depend on the production rate of radicals which is proportional to the product of $O_3$ and $H_2O$ if, as is often the case in this altitude

⏮ | ⏭

◀ | ▶

Back | Close

Full Screen / Esc

Printer-friendly Version

Interactive Discussion

range, $O_3$ photolysis is the dominant source of radicals (Daum et al., 1990; Tremmel et al., 1993; and Weinstein-Lloyd et al., 1996). Figure 3 illustrates the relationship between $H_2O_2$, $O_3$ and water vapor using all data obtained for altitudes >3500 m and [$NO_y$]<5 ppbv (with the exception of ferry transects to and from Veracruz). The slope of this line (0.0056 ppbv/ppmv$^2$) is similar to that observed in Nova Scotia (0.0054 ppbv/ppmv$^2$, Weinstein-Lloyd et al., 1996) and over the Northeastern United States (0.0050 ppbv/ppmv$^2$, Tremmel et al., 1993).

In the boundary layer, peroxide production is more complex, and depends on precursors, altitude and meteorology. We examined the trend in peroxide abundance when winds carried the urban plume over the L1 and L2 regions (Table 1). The best days for this transport, when the G-1 sampled air over T1 and T2, occurred on 18, 19, and 20th March. Figure 4 shows the mean peroxide concentration as a function of location for flights on these days. During this period the L5 transect was upwind of Mexico City and had the "cleanest" air (see Table 3). Concentrations at L5 are considered to be background levels for this comparison. Moving downwind from L5 a decreasing trend in peroxide concentration is observed. This range is small (0.3 ppbv) and the change in peroxide concentration is within the uncertainty of the measurement. Overall, the concentration of peroxide was low in background air, and its production suppressed over the entire Mexico City basin.

## 3.2.2 Peroxide in urban and power plant plumes

During this study, we identified 63 plume traverses characterized by an ozone increase of at least 20 ppbv. Figure 5a shows a typical plume traverse in the Mexico City basin on 20th March. There is a $NO_z$ plume (i.e., $NO_z=NO_y–NO_x$) coincident with the $O_3$ plume but no indication of an increase in $H_2O_2$ above background levels. Peroxide formation is inhibited by high $NO_x$ concentrations that effectively scavenge $HO_2$ radicals. Formation of $NO_z$ but not peroxides is characteristic of $O_3$ plumes that are formed under VOC limited conditions (Sillman, 1995; Kleinman et al., 2005b). There were only four ozone

plumes where we observed a peroxide increase above the detection limit of 0.27 ppbv. Three of these cases were observed at high (>4 km m.s.l.) altitude just east of the T1 site. An example for 19th March is shown in Fig. 5b. These plumes were characterized by low $NO_x$ (in this case <1 ppbv) and high $NO_z$ concentrations. $NO_z$ is representative of processed oxides of nitrogen (i.e., nitric acid). These few air masses had thus aged enough to allow for production of peroxide.

The concentration of $H_2O_2$ during a typical traverse of the Tula power/chemical processing facility is shown in Fig. 6. High $SO_2$ and $NO_y$ concentrations were always associated with flyovers in this region. Plumes were also characterized by dips in concentration for $O_3$ and $H_2O_2$ on at least five separate flights (i.e., $\Delta H_2O_2 = -0.6 \pm 0.1$ ppbv and $\Delta O_3 = -14 \pm 8$ ppbv) when the G-1 passed over the Tula facility. Ozone dips result from loss via reaction with NO. Cross-plume dips in peroxide have been observed previously for power plants (Jobson et al., 1998; Weinstein-Lloyd et al., 1998). The net destruction of peroxide near plume center has been attributed to the high $NO_x$ concentration, which inhibits peroxide production, coupled with peroxide loss by photolysis and reaction with OH.

### 3.2.3 Peroxide as a radical sink (i.e., $O_3$ vs. $2H_2O_2 + NO_z$)

Sillman has noted that the concentration of ozone, as a source of free radicals, should be related to the sum of peroxide and nitric acid, as a radical sink, independent of whether ozone formation is limited by VOC or $NO_x$ (Sillman, 1995; Sillman et al., 1998). We examined the relationship between $O_3$ and the sum of $NO_z + 2 H_2O_2$ for each transect described in Sect. 2.1. We include in Table 4 only those data for which $r^2 \geq 0.5$, indicative of a single air mass. Sillman et al. (1998) noted that there is little variation in this slope when observations are compared between rural locations and urban locations, where $O_3$ concentrations varied from 80 to 140 ppbv. The data in Table 4 confirm this observation, as there is no observable trend in slope between the source region and downwind regions. However, we did observe a distinct difference between the dry and wet period. On 21st March, the relative humidity changed abruptly from an aver-

age 30% to over 50%. After that date, the average $O_3$ versus ($NO_z+2\,H_2O_2$) slope (dry vs. wet) drops by 33% from 4.8±1.4 ($n$=12) to 2.9±0.8 ($n$=7). The direction of change is in agreement with the assumption in Sillman's work, that the correlation arises from a relation between radical production represented by $O_3$ and radical loss represented by $NO_z+2\,H_2O_2$. But radical production from $O_3$ is proportional to the product of $O_3$ and $H_2O$, and increasing $H_2O$ will result in a lower slope if the balance between production and loss of radicals is to be maintained. It is interesting that the relations predicted by Sillman occur in Mexico City, even though $O_3$ photolysis is not expected to be the dominant source of radicals (Volkamer et al., 2007)

## 3.2.4 Peroxides and particles

Hydrogen peroxide is largely responsible for oxidizing sulfur dioxide in clouds (Penkett et al., 1979; Calvert and Stockwell, 1983; Lind et al., 1987; Kleinman and Daum, 1991; Husain et al., 2000). Model calculations predict that a large fraction of the resulting sulfate is returned to the atmosphere as aerosol when clouds evaporate (Langner and Rodhe, 1991; Benkovitz et al., 2004). Observations of aerosol growth in a boundary layer with cloud coverage also indicate the importance of sulfur dioxide and hydrogen peroxide in generating a distribution of aerosol sizes (Wang et al., 2007). Unfortunately while in Mexico, the G-1 rarely flew in or near stable clouds, so this aspect of peroxide chemistry could not be investigated. However, we have examined the potential for aerosol formation based on the stoichiometry of the one-to-one reaction of $SO_2$ and $H_2O_2$ in the aqueous phase.

An evaluation of the aerosol mass spectrometer measurements aboard the G-1 showed that organic and nitrate aerosols dominate in the Mexico City basin with sulfate aerosol accounting for less than 20% (Kleinman et al., 2007); in sharp contrast to the eastern United States where sulfate dominates aerosol composition (Malm et al., 2004). Because peroxide concentrations were suppressed throughout the Mexico City basin, it seemed unlikely that aqueous-phase oxidation of $SO_2$ by peroxide contributed significantly to sulfate aerosol formation during the measurement period. Depending

on concentration, either $SO_2$ or $H_2O_2$ can be the limiting reagent to aerosol formation. In the MCMA, peroxide concentration varied from the detection limit to 3 ppbv, while $SO_2$, leaving aside plumes from Tula, varied from the detection limit to 24 ppbv. Taken as a whole, the mean value of $SO_2$ (3.0 ppbv) exceeded that of $H_2O_2$ (1.2 ppbv) making
5 peroxide the limiting reagent for sulfate formation (i.e., if liquid were present, peroxide would have been the limiting reagent to sulfate production). More specifically, when pairs of data points are examined we find that 60% of the observations were characterized by $SO_2$ greater than $H_2O_2$. In Fig. 7, we show a histogram of this observation with the highlighted area indicating the fraction of events when the $H_2O_2$ concentra-
10 tion was less than $SO_2$. Low humidity and a lack of available $H_2O_2$ meant there was little potential for aqueous phase sulfate aerosol production in the MCMA, supporting the observation of the low contribution of sulfate to the total apportionment of aerosol composition.

## 3.3  Surface measurements

15 ### 3.3.1  General observations and correlations with other species

The abundance of total hydroperoxide was determined for the period 13th–30th March with nighttime sampling beginning on 23rd March. We show the time series of total peroxide and related species for the entire measurement period in Fig. 8, and the composite diurnal profile of total peroxide in Fig. 9. On average, growth commences
20 around 9:00, reaching a maximum value of 1.3 ppbv between 14:00 and 15:00 LST. Peak peroxide values reached between 1 and 2 ppbv each afternoon, decayed slowly, and remained near 0.5 ppbv overnight. There were several episodes when we observed well-correlated events of peroxide and ozone after midnight (see the nights of 23rd, 24th, 25th and 27th March in Fig. 8). The time of day suggests that these are
25 due to advection events and/or boundary layer dynamics rather than local production.

### 3.3.2 Peroxides and peroxide precursors

In the absence of deposition and other losses, we would expect the abundance of peroxide to be related to solar intensity and the amount of its chemical precursors, peroxy radicals, ozone and water. Diurnal variations of these species are shown in Fig. 10. Mean ozone at this site peaks near 80 ppbv at 15:00 LST. Ozone, UVB and peroxy radicals rise at similar rates just after 07:00 LST, with the onset of peroxide growth lagging by 20–40 min. This period coincides with maximum $NO_x$ concentrations that are likely produced from local traffic emission into the shallow boundary layer. The very high concentrations of NO (the composite mean reaches 80 ppbv at 07:00 LST) should scavenge peroxy radicals and inhibit peroxide formation. The daytime peroxide profile is consistent with local photochemical production, peaking 1–2 h after solar noon, as seen in other locations (Lee et al., 2000 and references therein). Ozone and total hydroperoxide persist longer than peroxy radicals once photochemistry shuts off, as expected. Peak peroxide concentrations are low: the composite mean peaks at 1.2 ppbv at 14:00 LST. We observed low but nonzero peroxides at night, as discussed earlier. Peroxy radicals also remained measurable throughout most of the night at ∼2 pptv.

It was not uncommon to observe NO as high as hundreds of ppbv at this site, so we did not expect to see a simple correlation between peroxide and peroxy radicals. However, there were a few occasions when these species were well correlated during daytime production hours (Fig. 11). As expected, these were periods when $NO_x$ was low.

### 3.3.3 Dry vs. moist regime

As we have discussed in the aircraft observations, the measurement period was characterized by dry conditions until a rainy period began on 21st March. Rain events, indicated by the blue symbols in Fig. 8, were determined by precipitation collection on the roof of Tecamac University. Figure 8 shows that rain was rare prior to 3/21, but occurred almost daily after 3/21. At the T1 site, median midday relative humidity increased from

12% for the dry period (13–20 th March) to 26% for the wet period (21–30th March). In addition, LIDAR showed episodes during the wet period when aerosol layers formed aloft and descended to the minimum observable height (200 m a.g.l.), possibly as rain that evaporated before reaching the surface (Rich Coulter, private communication).

Although the peak ozone increased from 75 ppbv (dry) to 100 ppbv (wet), there was no significant increase in peak peroxide concentration (1.5 vs. 1.6 ppbv). Significant rainfall was associated with a dramatic decrease in peroxide, presumably due to wet scavenging on the afternoons of 26th March and 27th March (see Fig. 8). However, peroxides remained elevated during rainfall on the night of 25th March. Convection associated with the rain event may have mixed peroxides (and ozone) from aloft down to the surface.

### 3.3.4   T0-T1-T2 Transport periods

Fast et al. (2007) and Doran et al. (2007) have identified several days in March that were most favorable for transport of pollutants from MCMA to the T1 and T2 sampling sites. We have examined the abundance of ozone and peroxide during the days judged to be likely for transport (18–22, 24, and 30 March) and unlikely for transport (13–16 March). Mean peak ozone is significantly higher on transport days (ozone of 100 vs. 75 ppbv) but mean peak peroxide is essentially the same (median 1.7 vs. 1.6 ppbv). This is consistent with the discussion of the G-1 results, as the T1 site should experience excess ozone from high concentrations of precursors on transport days. Peroxide production does not accompany ozone formation on these days because the ozone is produced under VOC-limited conditions.

### 3.4   Comparison of ground and aircraft observations

The G-1 aircraft flew over the surface site numerous times, enabling us to compare peroxides at the T1 site with those observed on the aircraft. As noted in the experimental section, we were not able to measure speciated peroxides, so the comparison

of $H_2O_2$ observations from the G-1 with total soluble hydroperoxide at the surface site is only semi-quantitative. Peroxide concentrations were compared when the G-1 was within roughly 3 km of T1 and all of these data points were taken at altitudes <4.5 km. There is a reasonable correlation between the concentration of total peroxide at T1 and

5  $H_2O_2$ on G-1 over flights, as seen in Fig. 12. Concentrations observed at the T-1 site were lower than those observed on the G1, ostensibly due to depositional losses.

## 4  Discussion

In this section, we present details of the G-1 flights on 20th March as a case study. This day was selected because the standard G-1 flight legs were optimal for observations of

10  the progression of gas-phase reactions as the air moved from the source region over the surface sites.

### 4.1  20 March 2006 – a case study

On 20 March 2006, the winds were flowing from the southwest and had been since the previous day (shifting from the south to southwest on the previous day, 19 March).

15  Winds were strong and steady at ~6.5 m s$^{-1}$ ensuring that air over T1 and T2 originated in the source region earlier in the day (i.e., not a stagnation event). The G-1 morning flight consisted of a flight track over L3, L4, and L5, and the surface sites of T0, T1 and T2. The afternoon flight track was slightly different than previous days, only going over T1 and T2 (i.e., no over flight of T0). Although this is not a true Langrangian study, air

20  sampled at T1 would have originated at the T0 site 1.5 h earlier in the day, as calculated with an average wind speed of 6.5 m s$^{-1}$ and the 35 km distance between T0 and T1; the transit time from T0 to T2 was 3 h.

Shown in Fig. 13 are the time series plots for the trace gases (NO, $SO_2$, CO, and $O_3$) at the T1 surface site. At approximately 05:00 LST, concentrations of CO and NO

25  increase due to local emissions into the shallow boundary layer while $O_3$ concentra-

tions are near zero. Later in the morning, between 10:00 and 11:00 a.m., the boundary layer begins to rise and $O_3$ photochemistry proceeds, with $O_3$ reaching a maximum of 100 ppbv later in the day.

On 20th March, the G-1 flew over the T-1 site 3 times, twice in the morning and once in the afternoon. That morning the average $O_3$ concentrations observed on the G-1 as it flew over T1 were approximately 42 and 46 ppbv, in good agreement with the surface observation of 41 and 48 ppbv, respectively. By the afternoon, $O_3$ concentrations at T1 had risen to 98 ppbv and observations on the G-1 were in the same range (i.e., ∼90 ppbv). Although there was no formal side-by-side comparison of the ground and aircraft instruments, the flyovers provide confidence in the validity of the measurements.

During the morning flight and indicative of the source region, concentrations of CO and $NO_x$ were high over the L3, L4 and L0 transects, as shown in Fig. 14. Ozone concentrations were still low, below 50 ppbv over L3, L4, L5 and L0, partly due to titration with NO. The atmosphere was quite dry in the Mexico City source region with $H_2O$ concentrations <5 g/kg and peroxide concentrations were also low (∼1 ppbv). The afternoon flight shown in Fig. 15 shows that the ozone concentrations had doubled due to photochemistry and transport from the city. The peroxide concentrations had not changed significantly by the time the afternoon flight took place indicating that there was no enhanced production in the outflow of the MCMA. However, near Veracruz water vapor concentrations were significantly higher and $NO_x$ concentrations were low, as shown in the altitude profiles (Fig. 2), allowing for more production of peroxide with concentrations ≥3 ppbv.

Peroxide production rates were calculated from a constrained steady state box model similar to that used in a study of $O_3$ production in five US cities (Kleinman et al., 2005b). The observation that $H_2O_2$ concentrations do not increase downwind of the MCMA on 20th March is consistent with the calculations shown in Fig. 16. The calculations indicate that there was no new net production (i.e., production minus loss rates) in the MCMA region in the morning and thus no significant change in concentrations would

be observed by the time transects were flown over L1 and L2. For example, if the net production over L0 was in the range of $-0.1$ to $0$ ppbv $H_2O_2$ per hour and the travel time to L2 was 3 h (at the average wind speed of $6.5\,m\,s^{-1}$) then there would be no observable change in peroxide. By the afternoon, several rates for the net production of $H_2O_2 \geq 0.2$ ppbv/min were calculated for the L2 region, indicating that $NO_x$ levels had decreased and more significant formation of peroxide was beginning.

In contrast to the $H_2O_2$ production, significant $O_3$ production took place between the morning flight and the afternoon flight as evidenced by the increased concentrations observed over L1 and L2 (i.e., $>80$ ppbv) in Fig. 15. As the air mass moved from the MCMA region to the T1 and T2 sites there was a significant increase in ozone production efficiency (OPE, i.e., the number of molecules of ozone produced per molecule of $NO_z$) as well as improvement in correlation between $O_x$ and $NO_z$ from the morning to afternoon flights. Ozone production efficiencies for this day and the $NO_x/NO_y$ ratios for the corresponding transects are shown in Table 5. For the morning flight, all three transects had high $NO_x$ to $NO_y$ ratios indicative of fresh emissions due to local sources. By the afternoon flight, significant aging had taken place as the $NO_x$ to $NO_y$ ratio had decreased to 0.25. At this point, $NO_x$ concentrations in the area had been reduced sufficiently for more peroxide production to take place (i.e., see Fig. 16).

### 4.2  $H_2O_2$ Production rates by transect

All flights were segregated into regions as described in Sect. 2 and median constrained steady state (CSS) values are given in Table 6. No hydrocarbon samples were taken on L5 and therefore it is not included in the table (CSS calculations depend on the hydrocarbon samples). We note that the instantaneous production rate for peroxide is low over the first 3 regions of interest and increases slightly by the time the urban air mass has moved over the L2 region. The net production of peroxide is negative throughout most of the regions, with a positive net production at T2. Negative and low peroxide production rates have been observed previously in Phoenix, AZ (Nunnermacker et al., 2004) where they were attributed to the high $NO_x$ of the source region coupled with

a low rate of radical production due to the extremely dry climate. An interesting feature of the Mexico City data is that most of the radical production is not from $O_3$ in agreement with Volkamer et al. (2007). Overall, the total radical production rate, $Q$, is much higher for Mexico City than Phoenix. Therefore, the extremely high $NO_x$ concentrations effectively remove any radicals from peroxide forming pathways and inhibit peroxide formation in the Mexico City basin.

## 5   Conclusions

We have presented measurements of gas-phase hydroperoxides in and around Mexico City and Veracruz during March 2006, a region where to date there have been few field observations. Measured concentrations of hydroxymethyl hydroperoxide were at or near the detection limit for most of the program. This finding is not surprising given the absence of biogenic alkenes (Hewitt et al., 1990). Measured concentrations of hydrogen peroxide in the Mexico City basin were generally near 1 ppbv. The high humidity and low $NO_x$ concentrations near Veracruz consistently gave rise to the highest observed peroxide concentrations during the campaign.

The G-1 data set, in and downwind of Mexico City, contained 63 transects of plumes in which $O_3$ concentration increased by at least 20 ppbv. In only 4 of these plumes was there a significant increase in $H_2O_2$. The absence of $H_2O_2$ production indicates that in 59 cases, $O_3$ was formed in VOC limited conditions.

The high $NO_x$ conditions in the Mexico City Basin resulted in a calculated low or negative net production of hydrogen peroxide, with some evidence of production on the L2 transect farthest downwind from the source region. Because peroxides can persist in the atmosphere for several days, and may serve as a reservoir for free radicals, the production of high concentrations of hydrogen peroxide in the Mexico City basin would have important regional consequences. Although we did not observe the high peroxide concentrations predicted by some models, processed air at the T2 site displays significant ozone-forming potential, reflected by $NO_x/NO_y$ ratios near 0.3 and CO near

Printer-friendly Version

Interactive Discussion

230 ppbv. Additional peroxide production in this air mass as it travels farther downwind is expected. However, it would be difficult to predict its magnitude without a detailed model that includes dilution and additional precursors.

## References

Benkovitz, C. M., Schwartz, S., Jensen, M. P., Miller, M. A., Easter, R. C., and Bates, T. S.: Modeling atmospheric sulfur over the Northern Hemisphere during the Aerosol Characterization Experiment 2 experimental period, J. Geophys. Res., 109, D06208, doi:10.1029/2004JD004939, 2004.

Calvert, J. G. and Stockwell, W. R.: Acid generation in the troposphere by gas-phase chemistry, Environ. Sci. Technol., 17, 428A–443A, 1983.

Coulter, R.: private communication, Environmental Sciences Division, Argonne National Laboratory, Argonne, IL, 2007.

Daum , P. H., Kleinman, L. I., Hills, A. J., Lazrus, A. L., Leslie, A. C. D., Busness, K., and Boatman, J.: Measurement and interpretation of concentrations of $H_2O_2$ and related species in the upper Midwest during summer, J. Geophys. Res., 95, 9857–9871, 1990.

Doran, J. C., Abbott, S., Archuleta, J., et al.: The IMADA-AVER Boundary Layer Experiment in the Mexico City Area, B. Am. Meteorol. Soc., 79, 2497–2508, 1998.

Doran, J. C., Barnard, J. C., Arnott, W. P., Cary, R., Coulter, R., Fast, J. D., Kassianov, E. I., Kleinman, L., Laulainen, N. S., Martin, T., Paredes-Miranda, G., Pekour, M. S., Shaw, W. J., Smith, D. F., Springston, S. R., and Yu, X.-Y.: The T1-T2 Study: Evolution of Aerosol

Properties Downwind of Mexico City, Atmos. Chem. Phys., 7, 1585–1598, 2007, http://www.atmos-chem-phys.net/7/1585/2007/.

Fast, J. D., deFoy, B., Acevedo Rosas, F., Caetano, E., Carmichael, G., Emmons, L., McKenna, D., Mena, M., Skamarock, W., Tie, X., Coulter, R. L., Barnard, J. C., Wiedinmyer, C., and Madronich, S.: A meteorological overview of the Milagro field campaigns, Atmos. Chem. Phys., 7, 2233–2257, 2007, http://www.atmos-chem-phys.net/7/2233/2007/.

Hewitt, C.N., Kok, G.L., and Fall, R.: Hydroperoxides in plants exposed to ozone mediate air pollution to alkene emitters, Nature, 34, 56–57, 1990.

Husain, L., Ratigan, O. V., Dutkiewicz, V., Das, M., Judd, D. C., Khan, A. R., Richter, R., Bala-subramanian, R., Swami, K., and Waleck, C. J.: Case studies of the $SO_2$ + $H_2O_2$ reaction in clouds, J. Geophys. Res., 105, 9831–9841, 2000.

Jackson, A. V. and Hewitt, C. N.: Hydrogen peroxide and organic hydroperoxide concentrations in air in a eucalyptus forest in central Portugal, Atmos. Environ., 30, 819–830, 1996.

Jobson, B. T., Frost, G. J., McKeen, S. A., Ryerson, T. B., Buhr, M. P., Parrish, D. D., Trainer, M., and Fehsenfeld, F. C.: Hydrogen peroxide dry deposition lifetime determined from observed loss rates in a power plant plume, J. Geophys. Res., 103, 22 617–22 628, 1998.

Kleinman, L. I. and Daum, P. H.: Oxidant limitation to the formation of $H_2SO_4$ near a $SO_2$ source region, Atmos. Environ., Part A, 25, 2023–2028, 1991.

Kleinman, L. I., Daum, P. H., Lee, Y.-N., Nunnermacker, L. J., Springston, S. R., Weinstein-Lloyd, J., and Rudolph, J.: Sensitivity of ozone production rate to ozone precursors, Geophys. Res. Lett. 28, 2903–2906, 2001.

Kleinman, L. I.: The dependence of tropospheric ozone production rate on ozone precursors, Atmos. Environ., 39, 575–586, 2005a.

Kleinman, L. I., Daum, P. H., Lee, Y.-N., Nunnermacker, L. J., Springston, S. R., Weinstein-Lloyd, J., and Rudolph, J.: A comparative study of ozone production in 5 U.S. metropolitan areas. J. Geophys. Res. 110, D02301, doi:10.1029/2004JD005096, 2005.

Kleinman, L. I., Springston, S. R., Daum, P. H., Lee, Y.-N., Nunnermacker, L. J., Senum, G. I., Wang, J., Weinstein-Lloyd, J., Alexander, M. L., Hubbe, J., Ortega, J., Canagaratna, M. R., and Jayne, J.: The time evolution of aerosol composition over the Mexico City plateau, Atmos. Chem. Phys., 8, 1559–1575, 2008, http://www.atmos-chem-phys.net/8/1559/2008/.

Langner, J. and Rodhe, H.: A global 3-dimensional of the tropospheric sulfur cycle, J. Atmos.

## Hydroperoxides in MILAGRO, 2006

L. J. Nunnermacker et al.

Title Page

| Abstract | Introduction |
| Conclusions | References |
| Tables | Figures |

| ◄◄ | ►► |
| ◄ | ► |
| Back | Close |

Full Screen / Esc

Printer-friendly Version

Interactive Discussion

Chem., 13, 225–263, 1991.

Lee, J. H., Tang, I. N., and Weinstein-Lloyd, J. B.: Nonenzymatic method for the determination of hydrogen peroxide in atmospheric samples, Anal. Chem., 62, 2381–2384, 1990.

Lee, J. H., Chen, Y., and Tang, I. N.: Heterogeneous loss of gaseous $H_2O_2$ in an atmospheric sampling system, Environ. Sci. Technol., 25, 339–342, 1991.

Lee, J. H., Tang, I. N., Weinstein-Lloyd, J. B., and Halper, E. B.: An improved nonenzymatic method for the determination of gas-phase peroxides, Environ. Sci. Technol., 28, 1180–1185, 1994.

Lee, M., Heikes, B. G., O'Sullivan, D. W.: Hydrogen peroxide and organic hydroperoxide in the troposphere (a review), Atmos. Environ., 34, 3475–3494, 2000.

Lei, W., de Foy, B., Zavala, M., Volkamer, R., and Moline, L. T.: Characterizing ozone production in the Mexico City Metropolitan Area: a case study using a chemical transport model, Atmos. Chem. Phys., 7, 1347–1366, 2007,
http://www.atmos-chem-phys.net/7/1347/2007/.

Lind, J. A., Lazrus, A. L., and Kok, G. L.: Aqueous phase oxidation of sulfur (IV) by hydrogen peroxide, methyl hydroperoxide, and peroxy acetic acid, J. Geophys. Res., 92, 4171–4177, 1987.

Malm, W. C., Schichtel, B. A., Pitchford, M. L., Ashbaugh, L. L., and Eldred, R. A.: Spatial and monthly trends in speciated fine particle concentration in the United States, J. Geophys. Res., 109, D03306, doi:10.1029/2003JD003739, 2004.

Molina, L. T. and Molina, M. J.: Air Quality in the Mexico Megacity: An integrated assessment, Alliance for Global Sustainability Bookseries, Volume 2, edited by: Kauffman, J. M., Kluwer Academic Publishers, Boston, 384 pp, 2002.

Nunnermacker, L. J., Weinstein-Lloyd, J., Kleinman, L., Daum, P. H. Lee, Y. N., Springston, S. R., Klotz, P., Newman, L., Neuroth, G., and Hyde, P.: Ground-based and aircraft measurements of trace gases in Phoenix, Arizona (1998), Atmos. Environ., 4941–4956, 2004.

Penkett, S. A., Jones, B. M. R., Brice, K. A., and Eggleton, A. E. J.: The importance of atmospheric ozone and hydrogen peroxide in oxidizing sulfur dioxide in cloud and rain water, Atmos. Environ., 13, 123–137, 1979.

Sillman, S.: Use of $NO_y$, HCHO, $H_2O_2$, and $HNO_3$ as indicators for ozone-$NO_x$-hydrocarbon sensitivity in urban locations, J. Geophys. Res., 100, 14 175–14 188, 1995.

Sillman, S., He, D., Pippin, M., Daum, P. H., Imre, D. G., Kleinman, L., Lee, J. H., and Weinstein-Lloyd, J.: Model correlations for ozone, reactive nitrogen and peroxides for Nashville in com-

parison with measurements: Implications for $O_3$–$NO_x$ -hydrocarbon chemistry, J. Geophys. Res., 103, 22 629–22 644, 1998.

Sillman, S.: The erroneous use of receptor modeling to diagnose $O_3$– $NO_x$ -hydrocarbon sensitivity, Atmos. Environ., 33, 2289–2291, 1999.

Springston, S. R.: Research flights of the DOE RAF during Milagro, 2006, available at http://www.asp.bnl.gov/ASP_ST_mtg_pres_2006/Poster_Springston.pdf, 2006.

Tremmel, H. G., Junkermann, W., Slemr, F., and Platt, U.: On the distribution of hydrogen peroxide in the lower troposphere over the northeastern United States during late summer 1988, J. Geophys. Res., 98, 1083–1099, 1993.

Volkamer, R., Sheehy, P. M., Molina, L. T., and Molina, M. J.: Oxidative capacity of the Mexico City atmosphere. Part 1: A radical source perspective, Atmos. Chem. Phys. Discuss., 7, 5365–5412, 2007,
http://www.atmos-chem-phys-discuss.net/7/5365/2007/.

Wang, J., Daum, P. H., Kleinman, L. I., Lee, Y.-N., Schwartz, S. E., Springston, S. R., Jonsson, H., Covert, D., and Ellemna, R.: Observation of ambient aerosol particle growth due to in-cloud processes within boundary layers, J. Geophys. Res, 12, D14207, doi:10.1029/2006JD007989, 2007.

Watkins, B. A., Parrish, D. D., Buhr, M. S., Norton, R. B., Trainer, M., Yee, J. E., and Fehsenfeld, F. C.: Factors influencing the concentration of gas-phase hydrogen peroxide during the summer in Kinterbush, Alabama, J. Geophys. Res., 100, 22 841–22 851, 1995.

Weinstein-Lloyd, J., Daum, P. H., Nunnermacker, L. J., Lee, J. H., and Kleinman, L. I.: Measurement of peroxides and related species in the 1993 North Atlantic Regional Experiment. J. Geophys. Res. 101, 29 081–29 090, 1996.

Weinstein-Lloyd, J. B., Lee, J. H., Daum, P. H., Kleinman, L. I., Nunnermacker, L. J., Springston, S. R., and Newman, L.: Measurements of peroxides and related species during the 1995 summer intensive of the Southern Oxidants Study in Nashville, Tennessee, J. Geophys. Res, 103, 22 361–22 373, 1998.

**Table 1.** Flights when the peroxide instrument was operational.

| Flight | Start Time (LST) | Stop Time (LST) | General Description |
|--------|------------------|------------------|---------------------|
| 060315b | 15 : 00 : 41 | 18 : 15 : 36 | Weak Southeasterly flow |
| 060318a | 13 : 28 : 32 | 17 : 09 : 50 | Southerly flow |
| | | | No p.m. flight |
| 060319a | 09 : 58 : 40 | 12 : 52 : 41 | Strong South- Southwesterly flow |
| 060319b | 14 : 55 : 38 | 18 : 05 : 04 | Strong Southwesterly flow |
| 060320a | 09 : 32 : 50 | 12 : 17 : 22 | Strong South- Southwesterly flow |
| 060320b | 14 : 01 : 49 | 16 : 58 : 15 | Strong Southwesterly flow |
| 060322a | 09 : 30 : 46 | 12 : 23 : 30 | Moderate Southwesterly flow |
| | | | No p.m. flight |
| 060326a | 09 : 46 : 34 | 12 : 58 : 30 | Weak Westerly to Southwesterly flow |
| | | | No p.m. flight |
| 060327a | 10 : 57 : 37 | 14 : 09 : 50 | Weak Southerly flow |
| | | | No p.m. flight |

**Table 2.** Three Channel Peroxide Instrument operating parameters.

| Channel # | Scrubbing solution pH | Derivatizing Reagent | Species detected |
|---|---|---|---|
| 1 | pH 9 | p-hydroxyphenylacetic acid (POHPAA) | Total soluble hydroperoxide = $(H_2O_2 + MHP^*) + HMHP^{**}$ |
| 2 | pH 9 | Ferrous sulfate/benzoic acid (FeBA) | $H_2O_2 + HMHP$ |
| 3 | pH 6 | Ferrous sulfate/benzoic acid (FeBA) | $H_2O_2$ |

[*] Methyl hydroperoxide [**] Hydroxy methyl hydroperoxide

**Table 3.** Summary Statistics for G-1 Flights (15–27 March 2006)

| Species | L3 | | L4 | | L5 | | L0 | | L1 | | L2 | |
|---|---|---|---|---|---|---|---|---|---|---|---|---|
| | Mean | Max | Mean | Max | Mean | Max | Mean | Max | Mean | Max | Mean | Max |
| $H_2O_2$ (ppbv) | 1.2 | 2.2 | 1.1 | 2.5 | 1.6 | 3.0 | 1.4 | 2.3 | 1.3 | 2.5 | 1.4 | 3.2 |
| HMHP | 0.36 | 1.1 | 0.33 | 1.3 | 0.37 | 1.0 | 0.32 | 0.8 | 0.3 | 1.2 | 0.31 | 0.77 |
| $O_3$ (ppbv) | 71 | 156 | 64 | 179 | 50 | 76 | 69 | 98 | 57 | 90 | 55 | 72 |
| $NO_x$ (ppbv) | 16.4 | 50.0 | 17.7 | 85.7 | 3.3 | 41 | 23.4 | 69 | 3.3 | 10.3 | 2.3 | 6.6 |
| $NO_y$ (ppbv) | 26.6 | 68 | 27.8 | 117 | 8.8 | 58 | 33.7 | 92 | 8.8 | 20 | 7.0 | 13 |
| $NO_x/NO_y$ | 0.58 | 0.85 | 0.52 | 1.1 | 0.21 | 0.78 | 0.63 | 0.87 | 0.33 | 0.71 | 0.29 | 0.52 |
| CO (ppbv) | 609 | 1325 | 709 | 2914 | 284 | 1700 | 800 | 2048 | 257 | 456 | 231 | 324 |
| $SO_2$ (ppbv) | 3.6 | 27 | 3.4 | 24 | 1.0 | 8.3 | 3.6 | 15.5 | 1.2 | 5.5 | 2.3 | 17 |
| PCASP ($cm^{-3}$) | 2371 | 4685 | 2190 | 5838 | 1242 | 3978 | 2427 | 5730 | 1345 | 2703 | 1204 | 1966 |
| $H_2O$ ($g\,kg^{-1}$) | 6.0 | 8.8 | 6.0 | 8.5 | 5.9 | 7.9 | 5.5 | 8.0 | 5.1 | 7.9 | 4.7 | 7.5 |
| RH (%) | 51 | 80 | 51 | 79 | 50 | 81 | 47 | 74 | 47.2 | 83 | 43 | 83 |
| Temperature (°C) | 11.8 | 15.9 | 11.8 | 15.9 | 12.0 | 16.6 | 12.2 | 19.1 | 10.2 | 16.2 | 10.5 | 14.5 |

**Table 4.** Slope of the regression line of $O_3$ versus its termination products ($2[H_2O_2]+[NO_z]$).

| Flight | Region | Slope $[O_3]/(2[H_2O_2]+[NO_z])$ | $r^2$ | RH (%) |
|---|---|---|---|---|
| 060315b | L1 | 5.7 | 0.89 | 35±2 |
| | L3, L4, L5–L0 | 5.4 | 0.97 | 28±9 |
| 060318A | L1 | 4.0 | 0.55 | 24±10 |
| | L2 | 5.9 | 0.93 | 25±10 |
| 060319a | L3–L1 | 3.8 | 0.80 | 38±7 |
| | L0–L1 | 4.7 | 0.53 | 36±7 |
| | L2 | 5.6 | 0.80 | 39±7 |
| 060319b | L1 | 3.1 | 0.74 | 26±13 |
| | L2 | 5.0 | 0.50 | 27±9 |
| 060320a | L1 | 2.0 | 0.91 | 21±13 |
| 060320b | L1 | 5.9 | 0.94 | 26±9 |
| | L2 | 7.0 | 0.92 | 30±9 |
| 060322a | L0 | 1.5 | 0.71 | 61±7 |
| | L1 | 2.8 | 0.57 | 54±10 |
| | L2 | 3.3 | 0.52 | 74±12 |
| 060326a | L3, L4, L5–L1 | 2.3 | 0.73 | 70±4 |
| | L0 | 3.2 | 0.87 | 72±12 |
| 060327a | L3, L4–L1 | 4.1 | 0.90 | 66±9 |
| | L0–L1 | 3.4 | 0.78 | 65±9 |

Notes:
1)     Data for the entire transect were used to generate the slope and
2)     wet season begins on 060322a.

**Table 5.** Morning and afternoon OPEs on 20 March 2006.

| Flight Transect | OPE | $r^2$ | $NO_x/NO_y$ | $r^2$ |
|---|---|---|---|---|
| L0 | 5.2 | 0.82 | 0.85 | 0.99 |
| L1 | 5.0 | 0.94 | 0.75 | 0.99 |
| L2 | 4.0 | 0.62 | 0.72 | 0.96 |
| L1 | 6.7 | 0.98 | 0.44 | 0.94 |
| L2 | 7.4 | 0.95 | 0.25 | 0.91 |

Notes:
1)      Afternoon flights are listed below the single horizontal line and
2)      OPE and $NO_x/NO_y$ are slopes obtained from regressions of transect data.

**Table 6.** Mean values for several CSS calculations in the Mexico City basin.

| Parameter | Region | | | |
|---|---|---|---|---|
| | L3&L4 | L0 | L1 | L2 |
| $P_{hydrogen\,peroxide}$ = $H_2O_2$ production rate (ppbv h$^{-1}$) | 0.04 | 0.03 | 0.11 | 0.16 |
| Net $P_{hydrogen\,peroxide}$ (ppb h$^{-1}$) | −0.01 | −0.05 | 0.02 | 0.07 |
| $Q$ = radical production rate (ppbv h$^{-1}$) | 2.6 | 3.5 | 1.9 | 1.6 |
| % $O_3$ = fraction of radical produced from $O_3$ photolysis | 0.35 | 0.36 | 0.33 | 0.25 |
| $P_{O_3}$ = (ppbv h$^{-1}$) | 16 | 28 | 16 | 11 |
| $L_N/Q$ = fraction of radicals removed as $NO_x$ | 0.84 | 0.88 | 0.61 | 0.45 |
| $n$ | 22 | 15 | 35 | 30 |

Data obtained at altitudes <4000 m m.s.l.
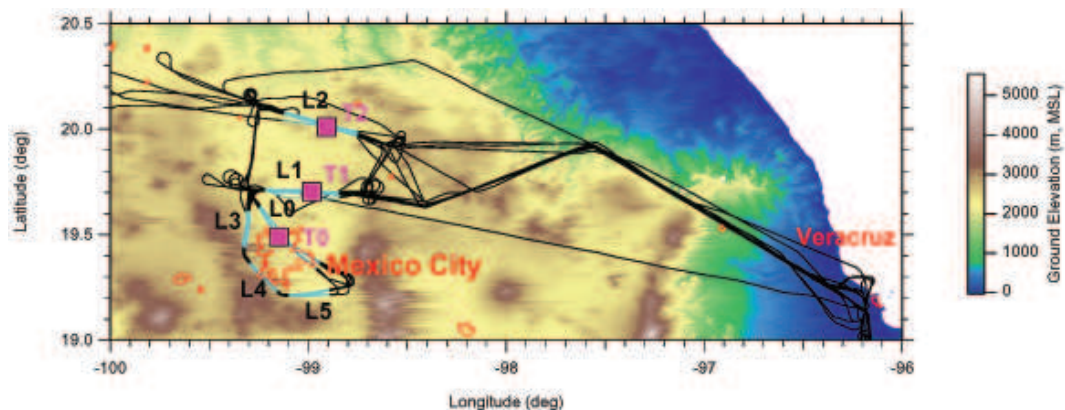
**Fig. 1.** Composite of all flight tracks (black lines) 15–27 March 2006. The Mexico City Metropolitan Area (MCMA) is indicated by the red outline within the flight legs. The blue lines indicate the flight legs in and around the MCMA (i.e., L0, L1, L2, L3, L4, and L5). The surface sites, T0, T1, and T2 are indicated by the square magenta symbols within the blue lines of the L0, L1, and L2 legs, respectively.
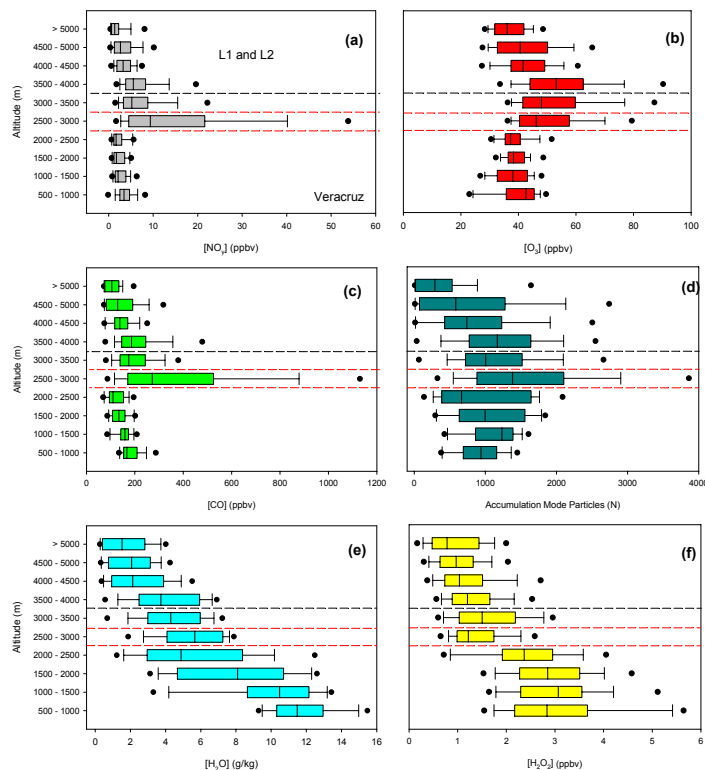
**Fig. 2.** Altitude distributions (MSL) showing the median (thin black line in box) concentrations of important trace gases during MILAGRO. Dashed red lines indicate measurements made on the Mexico City legs (i.e., L0, L3, L4, and L5). Dashed black line indicates that most measurements made above this line were in the L1 and L2 region. Boxes enclose 50% of the data, whiskers indicate the 10–90th percentile, and upper and lower limits (filled circles) are the 5th and 95th percentile of the data: **(a)**=$NO_y$, **(b)**=$O_3$, **(c)**=CO, **(d)**=Accumulation Mode Particles, **(e)**=Water Vapor, **(f)**=$H_2O_2$.

Title Page

Abstract | Introduction

Conclusions | References

Tables | Figures

◀◀ | ▶▶

◀ | ▶

Back | Close

Full Screen / Esc

Printer-friendly Version

Interactive Discussion
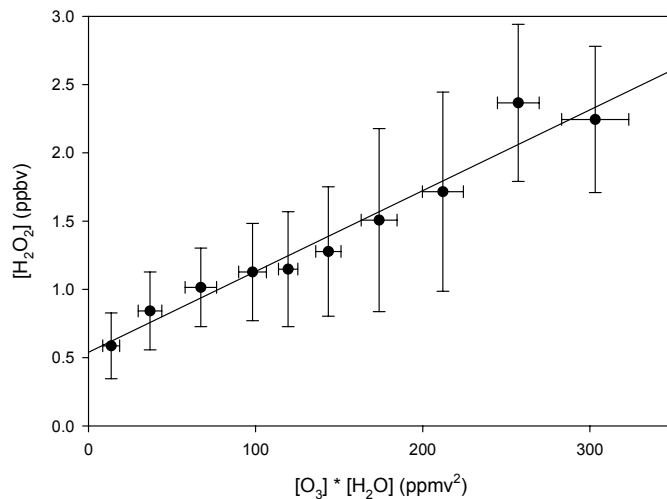
**Fig. 3.** Production of peroxide in the free troposphere at altitudes greater than 3500 m and [$NO_y$] less than 5 ppbv (data were binned as 10% increments of this set with circles indicating the average of the bin; error bars indicate the $1\sigma$ standard deviation of the binned data). Slope=0.0056, $r^2$=0.5, $n$=1974.
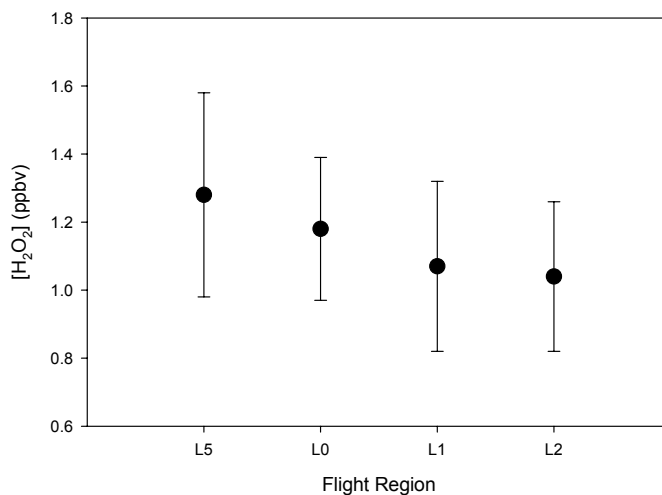
**Fig. 4.** Average peroxide concentration as a function of region in the Mexico City basin on southwesterly flow days. Error bars indicate the $1\sigma$ standard deviation of the averaged data for five flights on 18, 19, and 20th March.
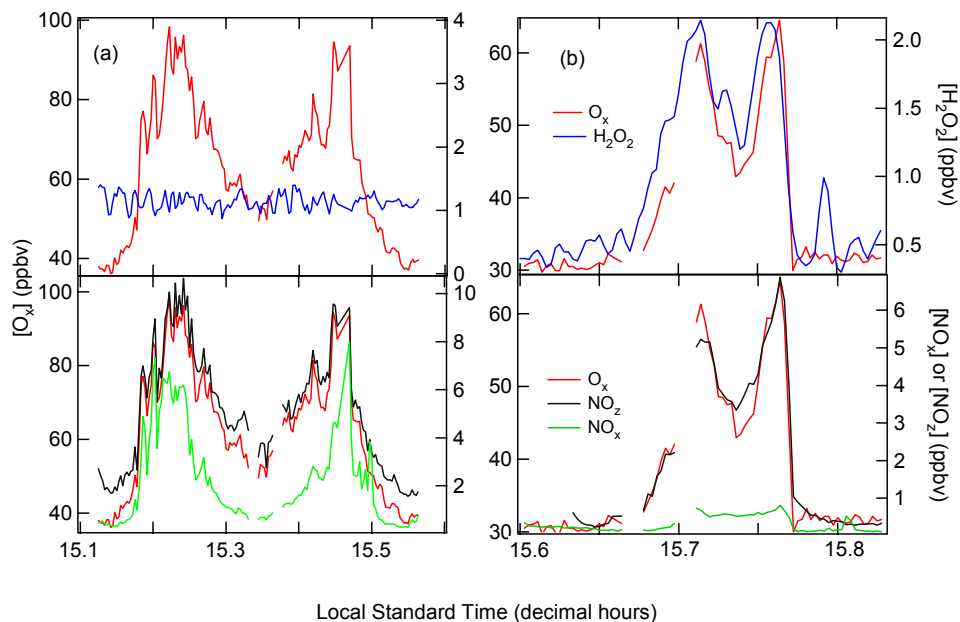
**Fig. 5.** Hydrogen peroxide in plumes: **(a)** No $H_2O_2$ production is observed on 20 March 2006, typical of the observations in the MCMA, **(b)** $H_2O_2$ production is observed on 19 March 2006 at an altitude of 4000 m. Color scheme is the same for (a) and (b): red=$O_x$, blue=$H_2O_2$, Black=$NO_z$, Green=$NO_x$.
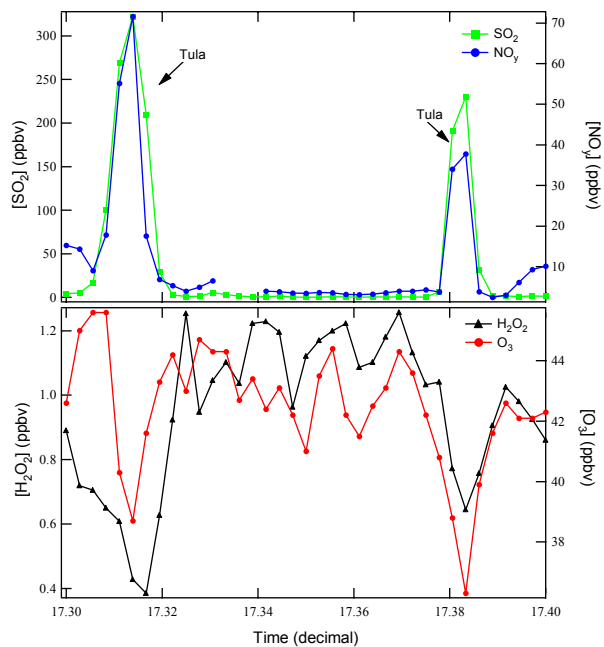
**Fig. 6.** Loss of ozone and hydrogen peroxide in the Tula facility stack plumes.
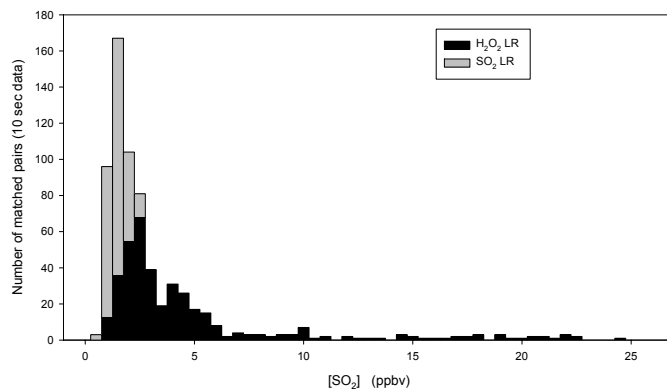
**Fig. 7.** $H_2O_2$ is the limiting reagent (LR) for 60% of the measurements when matched with $SO_2$ in the MCMA.
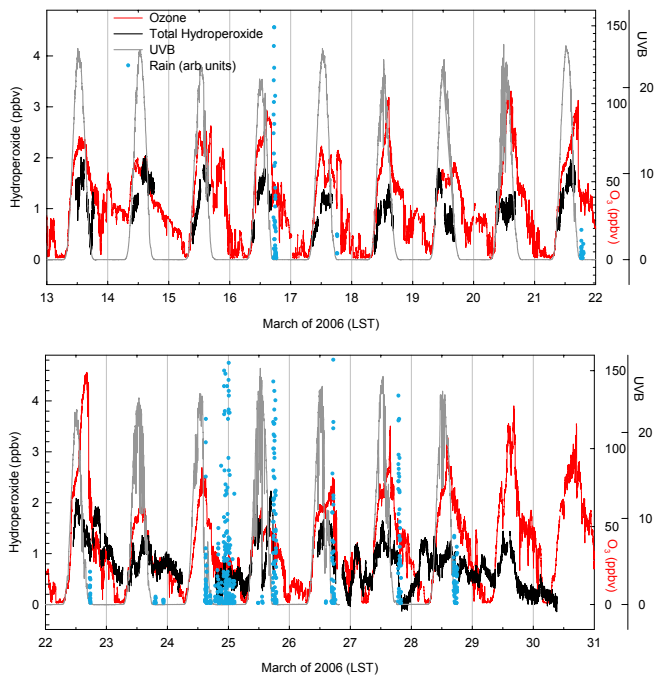
**Fig. 8.** Time series of total peroxide (in black) for the period 13–31 March 2006 at Tecamac University. Also shown are solar radiation (gray), ozone (red) and periods of measurable rainfall (blue) at this site.
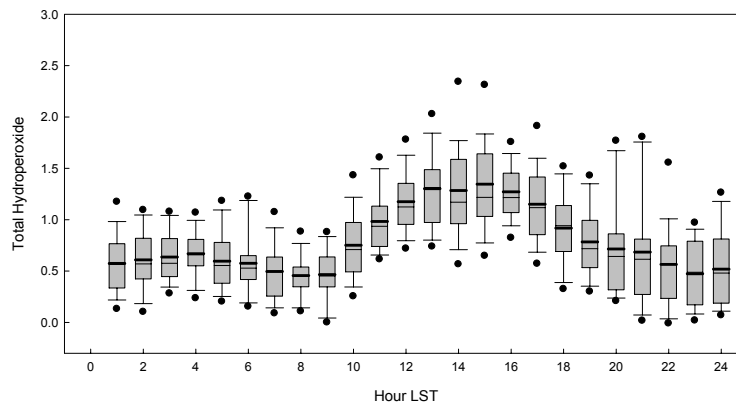
**Fig. 9.** Composite diurnal profile of total hydroperoxide determined at Tecamac University. Data have been binned into 1-h averages. The gray boxes enclose the central 50% of measurements; solid line is the median and dashed line is the mean; bars enclose all data in the 10th-90th percentile and symbols show the 5–95th percentile outliers.

Title Page

Abstract | Introduction

Conclusions | References

Tables | Figures

◄◄ | ►►

◄ | ►

Back | Close

Full Screen / Esc

Printer-friendly Version

Interactive Discussion
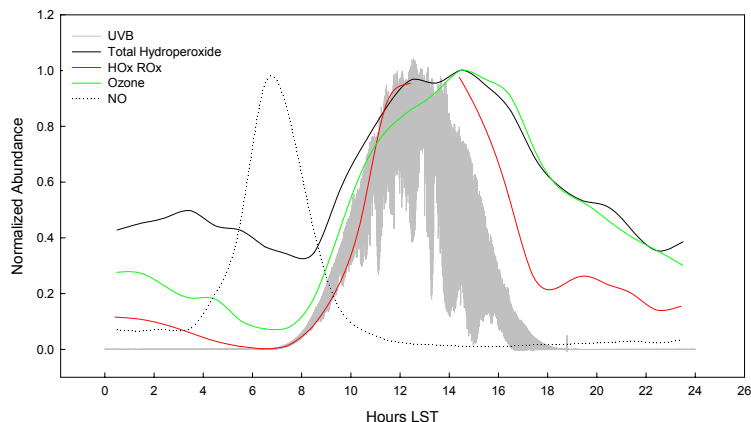
**Fig. 10.** Diurnal patterns for solar intensity, concentrations of total peroxide, ozone, NO, and peroxy radicals. Note that the concentrations have been scaled to illustrate the relationship between species. The trace gas data are mean hourly averages, which have been normalized to better compare the diurnal variations.
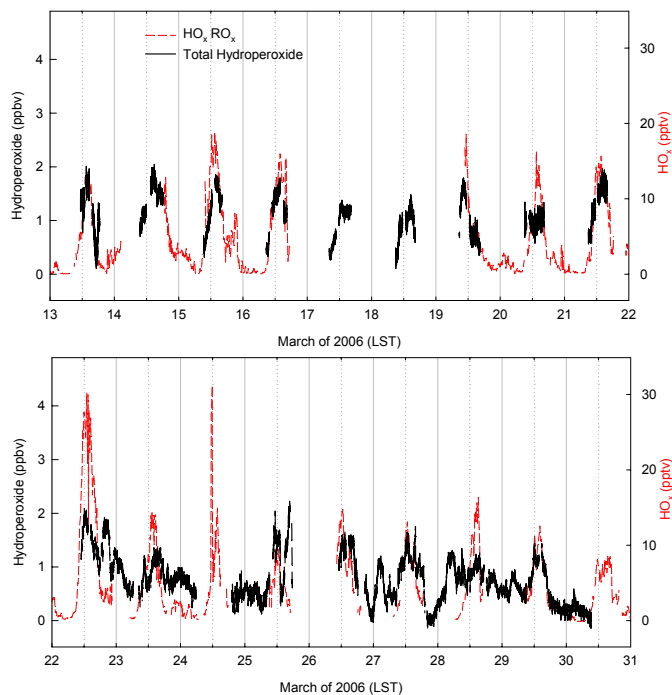
**Fig. 11.** Time series of hydroperoxides (black) along with $HO_2$ radicals (red) at Tecamac University.
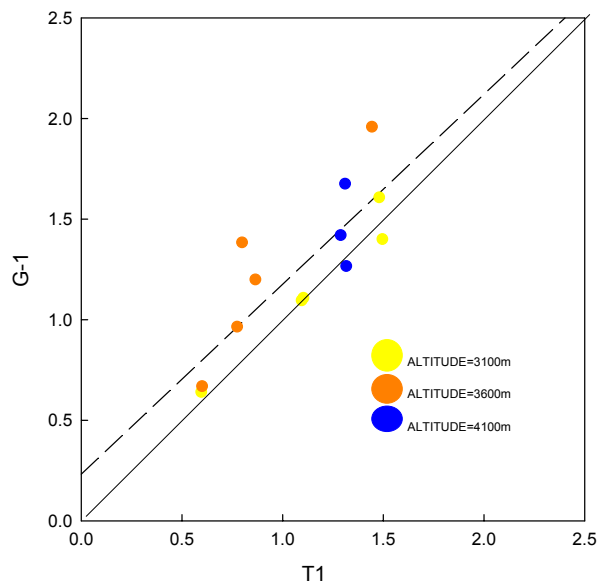
**Fig. 12.** Comparison of observed peroxides at the T1 surface site with the average obtained during flights over the site. The dotted line had the following regression: y=0.94[Peroxide] + 0.23 with a correlation coefficient $r^2$=0.68.
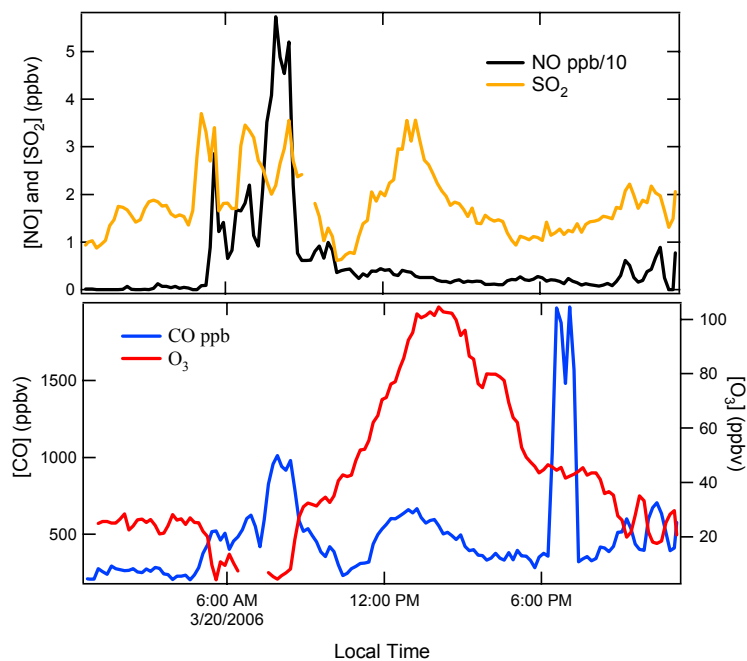
**Fig. 13.** Time series of trace gas observations on 20 March, at T1.
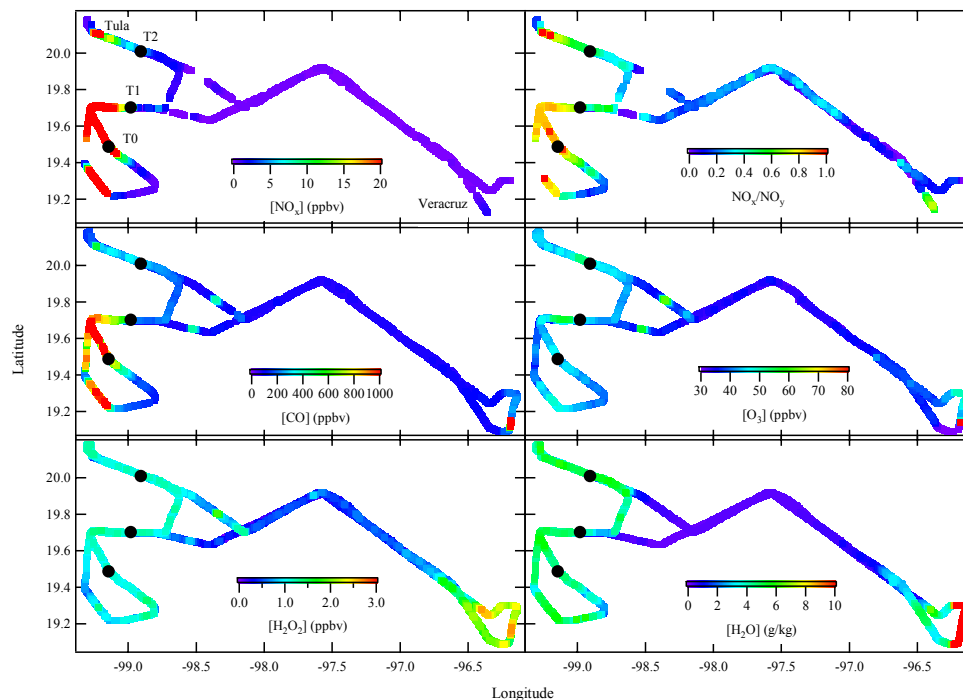
**Fig. 14.** Morning flight tracks on 20 March 2006. The color-coding on each flight track indicates trace gas concentrations.
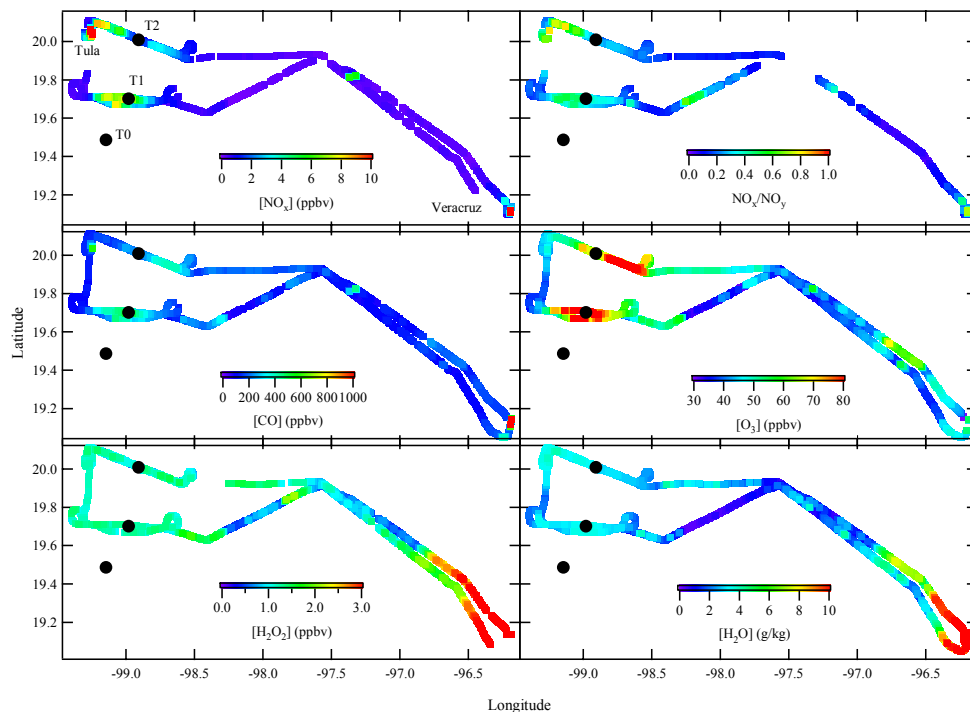
**Fig. 15.** Afternoon flight tracks on 20 March 2006. The color-coding on each flight track indicates trace gas concentrations.

Full Screen / Esc

Printer-friendly Version

Interactive Discussion
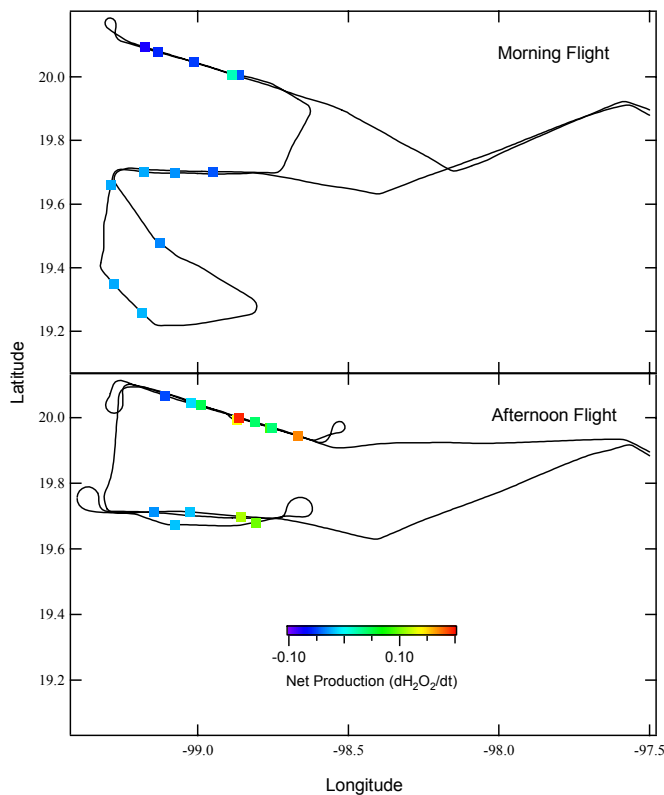


**Fig. 16.** Morning and afternoon net (i.e., production – loss) production of hydrogen peroxide on 20 March 2006 with each square indicating a hydrocarbon sampling location.